

## ORIGINAL ARTICLE

# Optical Properties of Electrodeposited CdMnS Thin Film Semiconductor Alloys for Optoelectronics Applications: Effect of Deposition Potential

A.N. Nwori<sup>a\*</sup>, N.L. Okoli<sup>a,b</sup>, N.A. Okereke<sup>a</sup>, I.E. Ottih<sup>a</sup> and L.N. Ezenwaka<sup>a</sup>

<sup>a</sup>Department of Industrial Physics, Faculty of Physical Science, Chukwuemeka Odumegwu Ojukwu University Uli, Anambra State, Nigeria.

<sup>b</sup>Department of Physics and Electronics, Faculty of Natural and Applied Sciences, Legacy University Okija, Anambra State, Nigeria

## KEYWORDS

Optoelectronics,  
Semiconductors,  
Bandgap, Electrodeposition,  
Photovoltaic

## ABSTRACT

Optical properties of semiconductor thin film alloys of cadmium manganese sulfide (CdMnS) deposited on fluorine-doped tin oxide (FTO) using an electrodeposition method is investigated for their possible optoelectronic device applications in this work. Cadmium sulphate, manganese sulphate and thiourea were starting materials used to source for sources of Cd, Mn and S ions respectively. Three electrodes configuration was utilized with the FTO serving as working electrode while Platinum rod and Ag/AgCl were used as counter and reference electrode respectively. The deposited thin films were characterized for their optical properties to determine their possible applications in optoelectronic devices. The result showed that the absorbance, absorption coefficient, refractive index and optical conductivity of the deposited thin films of CdMnS are high and influence by deposition voltage. The films have low reflectance and extinction coefficient in the visible and near-infrared regions of the electromagnetic spectrum. The bandgap energy of the films was found to be 2.6 eV, 2.7 eV, 2.8 eV, 2.7 eV and 2.5 eV for the films deposited at 1.6 V, 1.8 V, 2.0 V, 2.2 V and 2.4 V respectively. The structural and morphological properties of the films were also studied and discussed. These observed properties exhibited by films of CdMnS position them for optoelectronic applications especially in photovoltaic cells for solar energy harnessing.

## ARTICLE HISTORY

Received: May 13, 2022

Revised: June 15, 2022

Accepted: June 30, 2022

## 1 Introduction

Thin-film semiconductor materials have found quite copious applications in many modern electronic devices today. In optoelectronic device application in particular, thin-film semiconductors have demonstrated great applications in the development of many devices made of photovoltaic solar cells, light-emitting diodes (LEDs), photodetectors, optical fibre, light amplification by the stimulated emission of radiation (LASER) etc., [1].

The semiconductor thin films of cadmium sulfide (CdS) have been greatly utilized in the fabrication of window layer for photovoltaic solar cells with the absorber layers of CdTe, Cu<sub>2</sub>S, or CuInSe<sub>2</sub> regarding its high absorption coefficient in the

wavelength range of ultra-violet (UV) and visible (VIS) regions of the electromagnetic spectrum [2-4].

The conversion efficiency of 22.1% have been recorded for CdS/CdTe based solar cells and have been contributing to one of the current market leaders for thin-film photovoltaics (PV) cells, [5]. CdS thin films have been described as a very important n-type semiconductor material of group II-VI which have bulk bandgap energy of about 2.42 eV, [6]. This particular property has placed CdS thin films as one of the promising and potential materials for many electronics and optoelectronic device applications.

Regarding the potential applications of the CdS thin films for many device fabrications, efforts are being made by

\*CORRESPONDING AUTHOR | A.N. Nwori | [austine2010forreal@yahoo.com](mailto:austine2010forreal@yahoo.com)

© The Authors 2022. Published by JNMSR. This is an open access article under the CC BY-NC-ND license.

researchers to further explore its device applications and for high-performance improvement.

To achieve this, one way forward is the incorporation of foreign materials/elements into the crystals lattice of the semiconductor thin films through the process of alloying or control doping [7]. The use of materials that have inbuilt magnetic characteristics such as Manganese (Mn), Iron (Fe), Cobalt (Co), Nickel (Ni) etc. for this purpose have been tipped to demonstrate high-performance improvement to further explore the uses of CdS thin films when incorporated with ions of magnetic elements by allowing the possibility of tailoring their properties, [8, 9].

The high performance of ternary semiconductor thin films of CdS so obtained by incorporating these magnetic materials is known to stem from their peculiar properties arising through the process of the exchange interaction between the mobile spins of the conduction electrons and localized spins of the incorporated magnetic elements [10].

To that effect, Manganese-doped cadmium sulfide quantum dots fabricated using successive ionic layer adsorption and reaction (SILAR) method have been reported to demonstrate a higher power conversion efficiency ( $\eta$ ) of 2.85%, than the value of 2.11% obtained with bare CdS. The improved photovoltaic performance was attributed to the impurities from  $Mn^{2+}$  doping of CdS, which have an impact on the structure of the host material and consequently decreased the surface roughness, [11].

The Mn-doped CdS (Mn: CdS) and ZnS (Mn: ZnS) nanowires synthesized using chemical vapor deposition (CVD) method have been reported to open up opportunities for fundamental studies of optical, electrical, and magnetic properties in quasi-one-dimensional diluted magnetic semiconductor (DMS) systems which could lead to the development of nanoscale spintronic devices.

[12, 13]. reported the effect of manganese doping on bandgap energy of CdS nano-films deposited by electrodeposition method and found that bandgap energy of the CdS nanofilms increased with the increase of Mn percentage doping in the range of 2.02 eV to 2.35 eV. They observed that there was a decrease in band gap energy values of CdS films with different Mn percentage doping and attributed it to sp-d exchange interaction between the band electrons and localized d-electrons of Mn ions substituting  $Cd^{2+}$ . They suggested that such Mn-doped CdS films could serve as a suitable material for applications in thin films solar cells and other optoelectronic devices.

The thin films of  $Cd_{1-x}Mn_xS$  deposited at various manganese ion concentrations from 0 to 0.15 using the chemical bath method have been reported by [14]. The author stated that the thin films of  $Cd_{1-x}Mn_xS$  exhibited high transmittance of over 90%, for wavelength above the bandgap absorption edge and suggested that the high transmittance with consequent low

reflectance properties make the films ideal as a window material for heterojunction solar cells applications. Thin films of  $Cd_{1-x}Mn_xS$  ( $0 \leq x \leq 0.5$ ) synthesized using chemical deposition technique have also been reported by [15] to demonstrate good potentials for photoelectrochemical cells applications for conversion of light into electrical energy and can be engineered to cope with the maximum span of the solar spectrum.

In this article, we report the optical properties of CdMnS thin films semiconductor alloys deposited using an electrodeposition technique by varying deposition voltage for optoelectronic applications.

## 2 Materials and Method

### 2.1 Preparation of the CdMnS Thin Films

To prepare the ternary chalcogenide thin-film semiconductor alloys of CdMnS; Cadmium sulphate ( $CdSO_4 \cdot H_2O$ ), manganese sulphate ( $MnSO_4 \cdot H_2O$ ) and thiourea ( $CH_4N_2S$ ) were the main starting materials for the sources of Cd, Mn and S ions respectively. Ethylenediaminetetraacetic acid (EDTA) and sodium tri-sulphate ( $Na_2SO_3$ ) were used as a precipitating agent and supporting electrolyte respectively.

The method used is the electrodeposition method in which the principle of Faraday's law is utilized to deposit thin-film material on a conductive substrate. Three electrodes configuration setup which comprises of high purity platinum rod is used as a counter electrode, conductive fluorine-doped tin oxide (FTO) substrate used as working electrode, standard Ag/AgCl electrode used as reference electrode, 100 ml glass beaker was used as reaction bath, two digital multimeters (DT890C7 and Mastech: MY60) were used to measure current and voltage while potentiostat (model Zhaoxin: RXN-3010D) was as DC supply unit.

To deposit the CdMnS thin films; 10 ml of 0.2 M  $CdSO_4 \cdot H_2O$ , 10 ml of 0.1 M ( $CH_4N_2S$ ), 5 ml of 0.025 M ethylenediaminetetraacetic acid (EDTA) as a complexing agent and 10 ml of 0.05 M  $Na_2SO_3$  as supporting electrolyte were used to complexes the ions of Cd and S. Thereafter, 10 ml of 0.1 M  $MnSO_4 \cdot H_2O$  was added to the bath containing the solution of the sources  $Cd^{2+}$  and  $S^{2-}$  ions.

The setup was completed by inserting the electrodes in the reaction bath containing the solution and thin films of CdMnS were seen depositing on the conductive FTO glass substrate by passing a current through the solution at a controlled voltage of 1.6 Volts for 60 seconds.

The process was repeated four more times by varying potentials (voltages) in the order of 1.6 V, 1.8 V, 2.0 V, 2.2 and 2.4 V while the concentration of the reagents including deposition time of 60 seconds was kept constant. The five samples of the CdMnS thin films fabricated are presented in table 1.

Table 1: Preparation of CdMnS thin films by varying deposition voltage

Bath Name	CdSO <sub>4</sub> .H <sub>2</sub> O		MnSO <sub>4</sub> .H <sub>2</sub> O		CH <sub>4</sub> N <sub>2</sub> S		EDTA		Na <sub>2</sub> SO <sub>3</sub>		Time (s)
	Conc. (Mol)	Vol. (ml)	Conc. (Mol)	Vol. (ml)	Conc. (Mol)	Vol. (ml)	Conc. (Mol)	Vol. (ml)	Conc. (Mol)	Vol. (ml)	
	0.2	10	0.1	10	0.1	10	0.025	5.0	0.05	10	60.00
Deposition Voltage (V)	1.60		1.80		2.00		2.20		2.40		

## 2.2 Characterization of the Deposited CdMnS Thin Films

The deposited thin films of CdMnS were characterized for their thickness and optical properties to determine their possible areas of device applications using the gravimetric method and UV-VIS spectrophotometric technique. The thickness of the films was estimated using the relation as given by [16-18]:

$$t_f = \frac{M}{\rho S_a} \quad (1)$$

where M represents the mass of the thin films deposited on the surface of the FTO glass substrate, which was calculated via the expression:

$$M = m_2 - m_1 \quad (2)$$

where m<sub>2</sub> is the mass of the FTO glass substrate after the film deposition, m<sub>1</sub> is the mass of plain FTO glass substrate before the film is deposited, ρ is the bulk average densities (g/cm<sup>3</sup>) of CdS and Mn, S<sub>a</sub> is the surface area of the substrate the thin films were deposited.

The optical properties were determined using UV-VIS Spectrophotometer (model: U756S-19-018) by measuring the absorbance of the deposited thin films. The absorbance measurement was carried out in the wavelength range of 200 nm to 1100 nm at an interval of 1 nm and a delay time of zero seconds.

The measured absorbance values of the films were used to calculate other optical properties using appropriate formula/equations. To that effect, the percentage transmittance of the films was calculated using the formula as given by [19]:

$$T = 10^{-A} \quad (3)$$

where A is the measure absorbance of the films.

**Reflectance:** the percentage reflectance of the films was calculated using the conservation law as given by [20]:

$$A + T + R = 1 \quad (4)$$

Rearranging gives:

$$R = 1 - (A + T) \quad (5)$$

where A and T are the measured absorbances and calculated transmittance from equation (3).

**Absorption coefficient (α):** this property for the deposited thin films of CdMnS was estimated using the relation given by [21, 22]:

$$\alpha = \frac{1}{t_f} (\ln T^{-1}) \quad (6)$$

where t<sub>f</sub> is the film thickness and T is the transmittance of the films.

**Extinction coefficient (k):** the extinction coefficient k of the films was calculated from the relation given by [23]:

$$k = \frac{\alpha \lambda}{4\pi} \quad (7)$$

where α is the absorption coefficient of the films and λ is the wavelength of light.

**Refractive index (n):** the refractive index was calculated via the relation as given by [24]:

$$n = (1 + \sqrt{R}) / (1 - \sqrt{R}) \quad (8)$$

where R is the reflectance of the films.

**Optical conductivity:** The optical conductivity of the deposited thin films was calculated using the relation given by [25, 26]:

$$\sigma = \alpha \eta C / 4\pi \quad (9)$$

Where α is the absorption coefficient, η is the refractive index and C is the speed of light.

**Bandgap energy (E<sub>g</sub>):** the bandgap energy of the deposited thin films of CdMnS was estimated from the plot of Tauc relation as given [27]:

$$(h\nu = A(h\nu - E_g)^r \quad (10)$$

Where r is known as transition factor which is 1/2 for direct band transition, 2 for indirect band electronic transition, 3/2 for direct forbidden transition and 3 for indirect forbidden transition, A is a constant known as band trailing parameter, α is the absorption coefficient, h is the Plank constant and ν is the frequency.

The structural properties of the films were evaluated using EMPYREAN Diffractometer with a Cu-Kα radiation (λ = 0.15406 nm). The measurement was done at scan step size of

0.0262606 degree and two theta angle range of 5 degrees to 75 degrees to obtain diffraction profiles of the films. Libraries from the X'Pert High Score Plus software were used to match the measured XRD patterns.

The micrograph/morphology of the deposited thin films was characterized using MIRA 3 TESCAN scanning electron microscopy and set at 20,000 magnifications.

### 3 Results and Discussions

#### 3.1 Thin film thickness studies

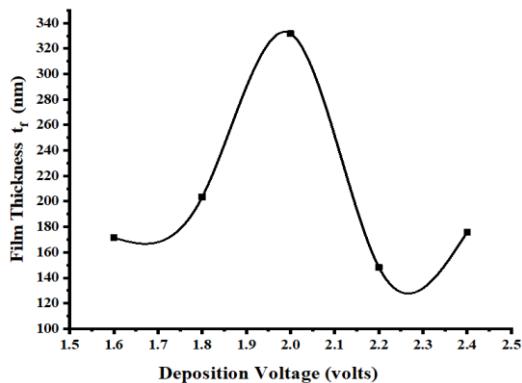


Figure 1: Graph of thin film thickness against deposition voltage for the CdMnS thin films

Figure 1 is the plot of the film thickness against deposition voltage for the deposited thin films of CdMnS. The figure showed that the thickness of the deposited CdMnS thin films initially increased as the deposition voltage increased up to the maximum thickness of 332 nm and then decreased as deposition voltage increased past 2.0 Volts. The maximum value of the film thickness (332 nm) was obtained at a deposition voltage of 2.0 Volts while the minimum thickness (140 nm) occurred at a deposition voltage of 2.26 Volts.

#### 3.2 The Optical Properties of the Films

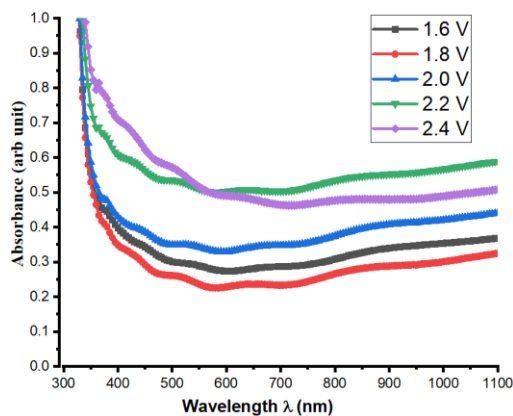


Figure 2: Graph of absorbance against wavelength for the CdMnS thin films deposited

Graph of spectral absorbance against wavelength for the deposited thin films is displayed in figure 2. From the figure, it is observed that the spectral absorbance of the deposited CdMnS thin films is high and increases as deposition voltage increased, throughout the visible and near-infrared (Vis & NIR) regions of the electromagnetic spectrum. The films have spectral absorbance in the range of 0.3 to 1.0 in two regions. The high absorbance value exhibited by the films in the VIS and NIR regions positions them for photovoltaic cell application.

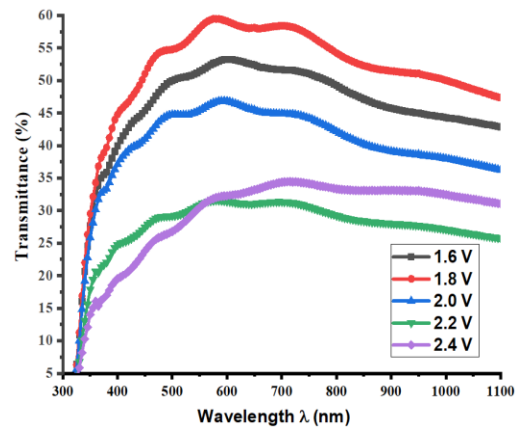


Figure 3: Graph of transmittance against wavelength for the CdMnS thin films deposited

The graph of percentage transmittance versus wavelength for the films is displayed in figure 3. The figure showed that the transmittance of the deposited CdMnS thin films decreases as deposition voltage increases throughout VIS and NIR regions. The film deposited at the voltage of 1.8 Volts has the highest transmittance value of 60% in these regions while films deposited at voltages of 2.2 and 2.4 Volts have the lowest transmittance in the range of 20-30% throughout Vis and NIR regions.

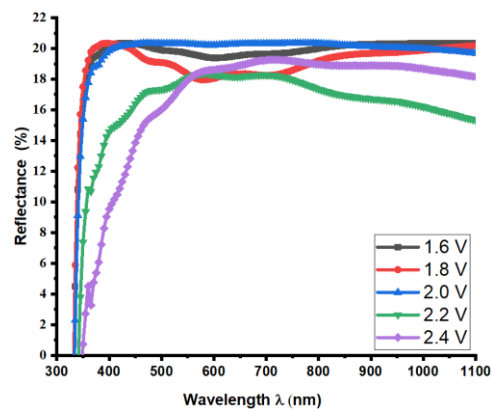


Figure 4: Graph of Reflectance against wavelength for the CdMnS thin films deposited

The graph of reflectance against wavelength for the deposited thin films of CdMnS is presented in figure 4. The figure indicates that the deposited CdMnS thin films have low reflectance throughout VIS and NIR regions. The range of percentage reflectance of the films in these regions is 0% to 20%. This low reflectance value of the films affirms the good application of the films in Photovoltaic cell development for solar energy harnessing.

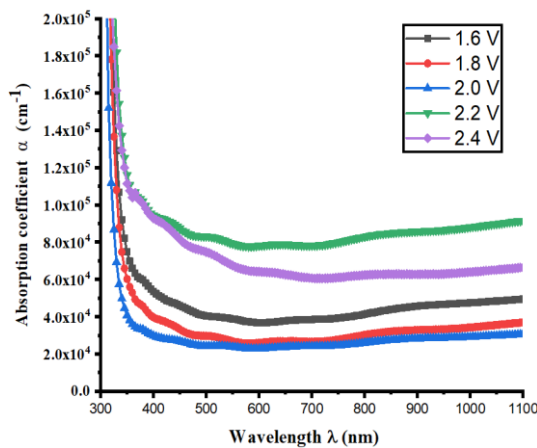


Figure 5: Graph of Absorption coefficient ( $\alpha$ ) against wavelength for the CdMnS thin films deposited

The plot of absorption coefficient as a function of wavelength for the deposited thin films is presented in figure 5. The figure showed that the deposited thin films of CdMnS have high absorption coefficient to the order of  $10^4$ - $10^5$   $\text{cm}^{-1}$  throughout VIS and NIR regions. The value of the absorption coefficient is also found to initially decrease with an increase in deposition voltage up to 2.0 V and then increase as deposition voltage increased further throughout the VIS and NIR regions.

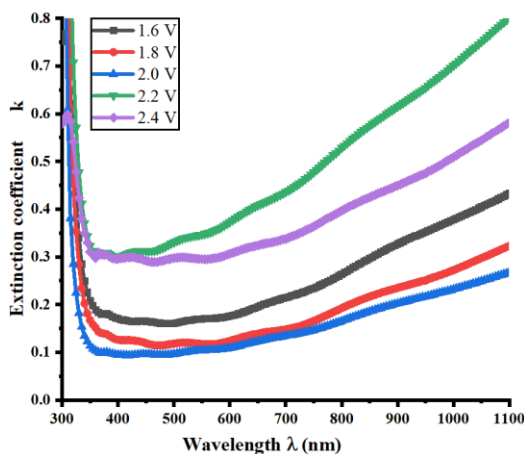


Figure 6: Graph of Extinction coefficient ( $k$ ) against wavelength for the deposited CdMnS thin films

Figure 6 is the plot of the extinction coefficient against wavelength for the deposited thin films. The plot showed that

the extinction coefficient of the films is pretty low in the range of 0.1 to 0.8 with a lower value in the range of 0.1 to 0.5 in the Vis region while higher values of up to 0.8 occurred in the NIR and part of ultra-violet regions. The value of extinction coefficient of the films was also found to initially decrease with an increase in deposition voltage but increased as the voltage increased past 2.0 V.

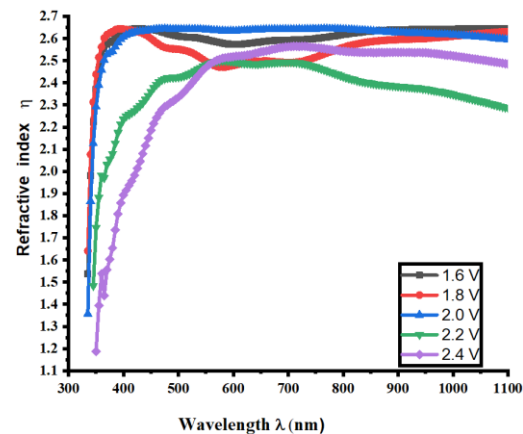


Figure 7: Graph of Refractive index ( $\eta$ ) against wavelength for the deposited CdMnS thin films

The graph of the refractive index against wavelength for the deposited thin films of CdMnS is displayed in figure 7. The graph indicates that the films have a high value of refractive index throughout the VIS and NIR regions of the electromagnetic spectrum. The range of values of the refractive index of the films is in the range of 2.3 to 2.65 and decreases as deposition voltage increases.

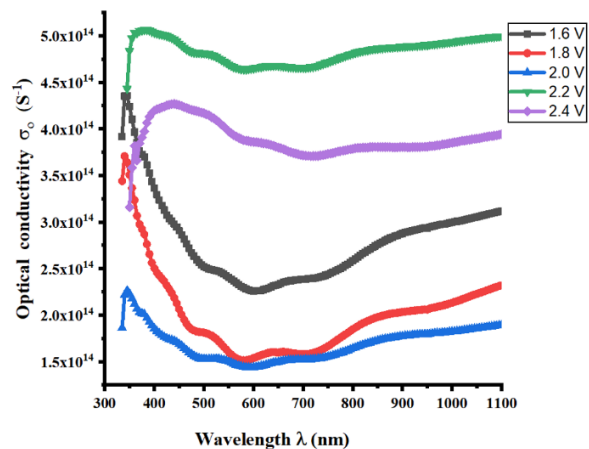


Figure 8: Graph of Optical conductivity ( $\sigma_0$ ) against wavelength for the deposited CdMnS thin films

Figure 8 is the plot of the optical conductivity against wavelength for the deposited thin films. The graph indicates that the films generally exhibit high optical conductivity throughout the Vis and NIR regions of the electromagnetic spectrum. The films initially showed a decrease in the value of



optical conductivity as deposition voltage increased but suddenly increased to higher values for the films deposited at voltages of 2.2 and 2.4 Volts.

Figure 10 is a plot of  $(\alpha h\nu)^2$  against photon energy ( $h\nu$ ) to determine the direct bandgap energy of the deposited thin films of CdMnS. From the plot, the bandgap energy extrapolated on the energy axis at  $(\alpha h\nu)^2$  equal to zero for the deposited films was observed to increase with an increase in deposition voltage.

The values of the bandgap energies for each of the deposited films were observed to be 2.6 eV, 2.7 eV, 2.8 eV, 2.7 eV and 2.5 eV for the films deposited at 1.6 V, 1.8 V, 2.0 V, 2.2 V and 2.4 V respectively. This result also showed that incorporation of manganese ions into CdS film crystals to form CdMnS have led to an increase in bandgap energy with maximum value obtained at deposition voltage of 2.0 V.

### 3.3 Structural Properties of the Deposited CdMnS Thin Films

Figure 9 is the plot of the XRD patterns of the films of CdMnS deposited at 2.0 V and 2.4 V. The XRD patterns reveal that the deposited films are crystalline with sharp peaks which occurred at two theta positions that correspond to crystalline planes (001), (110), (020), (121), (102) and (220). The patterns matched almost well with the JCPDS data for CdS and MnS as seen inserted in the plot of the XRD patterns. The crystallite size ( $D$ ), dislocation density ( $\delta$ ) and the micro-strain ( $\epsilon$ ) of the films were calculated using the relations as given respectively by [28-30]:

$$D = \frac{k\lambda}{\beta \cos\theta} \quad (11)$$

$$\delta = \frac{1}{D^2} \quad (12)$$

$$\epsilon = \frac{\beta}{4 \tan\theta} \quad (13)$$

Where  $k$  is called shape factor,  $\lambda$  is the x-ray wavelength of Cu-K $\alpha$  radiation,  $\beta$  is full width at half maximum (FWHM) and  $\theta$  is the Bragg's angle. The calculated values of these parameters at two theta sharp positions with their average values are tabulated in table 2. The average crystallite size of the films is found to decrease with an increase in deposition voltage while dislocation density and micro-strain displayed increasing trend. These behaviour of the calculated parameters can be attributed to decreasing trend in the film thickness from deposition voltage of 2.0 V.

The degree of crystallinity of the films calculated using the relations as given by [31, 32]:

$$\text{Crystallinity} = \frac{\text{Total area of crystalline peaks}}{\text{The full size of all peaks}} \times 100\% \quad (14)$$

The calculated values of degree of crystallinity are 91.41% and 57.79% for the films deposited at 2.0 V and 2.4 V respectively. These percentage values further confirmed the crystalline nature of the deposited thin films of CdMnS under the prescribed conditions for a desired application.

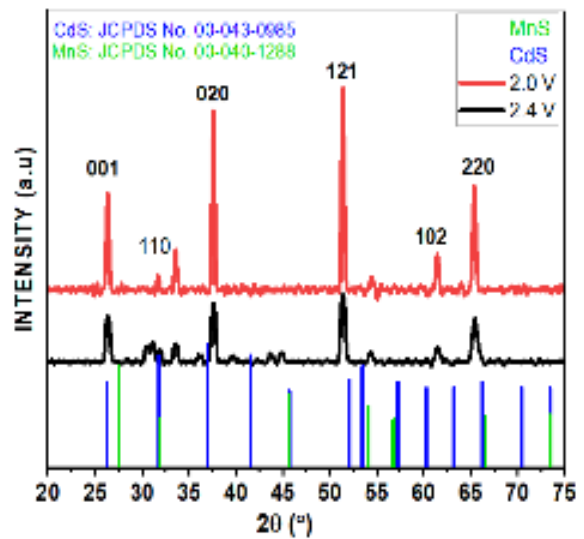


Figure 9: XRD patterns of the deposited CdMnS thin films

Table 2: Average crystallite size, dislocation density and micro-strain for deposited CdMnS thin films

Samples	2 theta (deg)	h k l	Crystallite size D (nm)	Average crystallite size, D (nm)	Dislocation density $\delta$ (lines/nm <sup>2</sup> )	Av. dislocation Density, $\delta$ (lines/nm <sup>2</sup> )	Micro-strain ( $\epsilon$ )	Av. micro-strain ( $\epsilon$ )
2.0 V	26.35	0 0 1	24.78	25.54	$1.62 \times 10^{-3}$	$1.53 \times 10^{-3}$	$6.13 \times 10^{-3}$	$3.87 \times 10^{-3}$
	33.57	1 1 0	25.47		$1.54 \times 10^{-3}$		$4.71 \times 10^{-3}$	
	37.60	0 2 0	25.75		$1.50 \times 10^{-3}$		$4.17 \times 10^{-3}$	
	51.38	1 2 1	26.16		$1.46 \times 10^{-3}$		$3.05 \times 10^{-3}$	
	61.45	1 0 2	27.03		$1.36 \times 10^{-3}$		$2.51 \times 10^{-3}$	
	65.38	2 2 0	24.04		$1.72 \times 10^{-3}$		$2.66 \times 10^{-3}$	

2.4 V	26.36	0 0 1	16.14	16.56	$3.83 \times 10^{-3}$	$3.69 \times 10^{-3}$	$9.41 \times 10^{-3}$	$5.94 \times 10^{-3}$
	33.57	1 1 0	17.35		$3.31 \times 10^{-3}$		$6.91 \times 10^{-3}$	
	37.61	0 2 0	17.00		$3.45 \times 10^{-3}$		$6.32 \times 10^{-3}$	
	51.39	1 2 1	17.26		$3.35 \times 10^{-3}$		$4.63 \times 10^{-3}$	
	61.48	1 0 2	17.16		$3.39 \times 10^{-3}$		$3.94 \times 10^{-3}$	
	65.44	2 2 0	14.45		$4.78 \times 10^{-3}$		$4.43 \times 10^{-3}$	

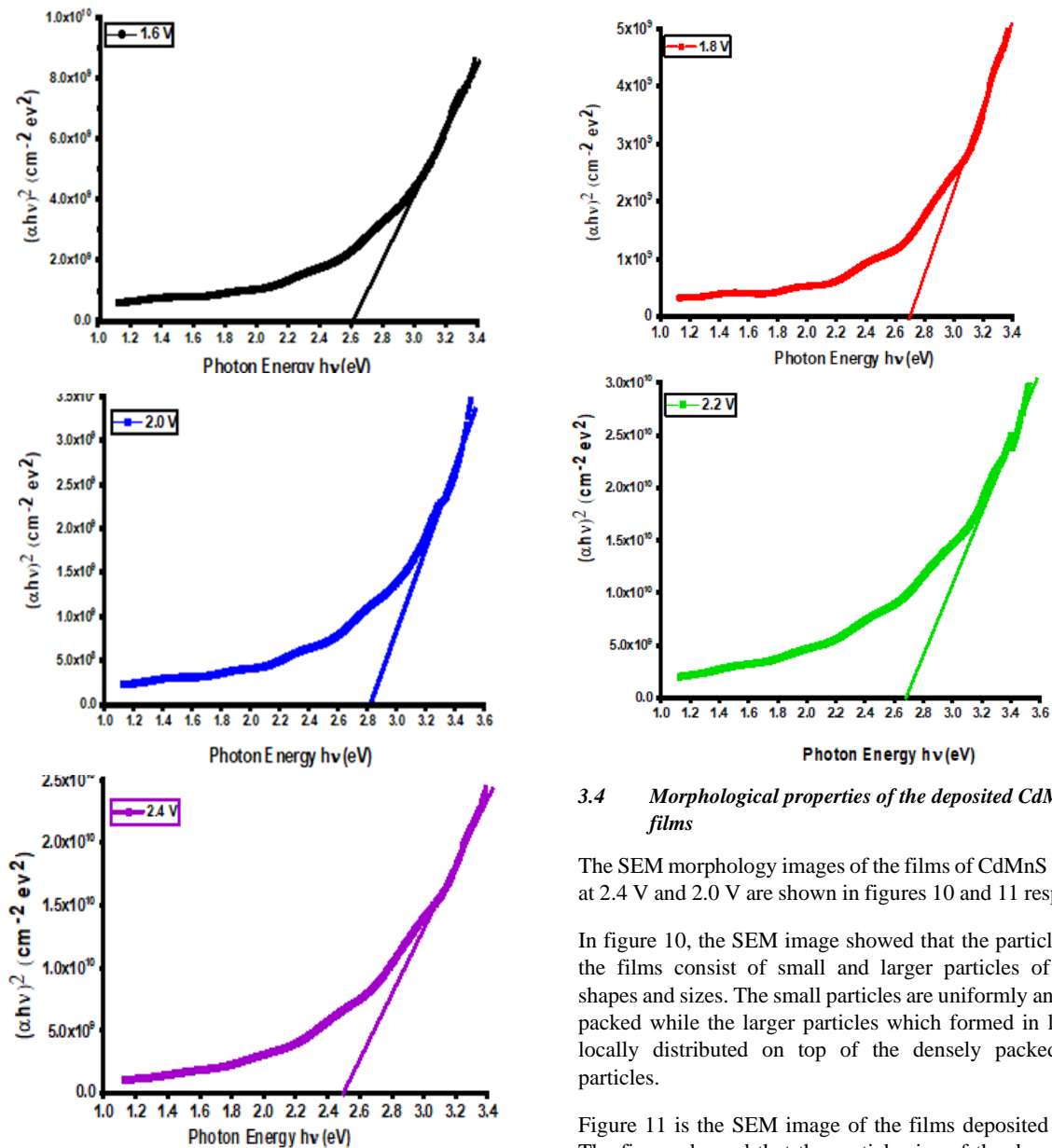


Figure 10: Graphs of  $(\alpha h\nu)^2$  against Photon energy ( $h\nu$ ) for the deposited CdMnS thin films

### 3.4 Morphological properties of the deposited CdMnS thin films

The SEM morphology images of the films of CdMnS deposited at 2.4 V and 2.0 V are shown in figures 10 and 11 respectively.

In figure 10, the SEM image showed that the particle sizes of the films consist of small and larger particles of irregular shapes and sizes. The small particles are uniformly and densely packed while the larger particles which formed in lumps are locally distributed on top of the densely packed smaller particles.

Figure 11 is the SEM image of the films deposited at 2.0 V. The figure showed that the particle size of the deposited thin films is of spherical in shape and uniformly deposited on the surface of the substrate.

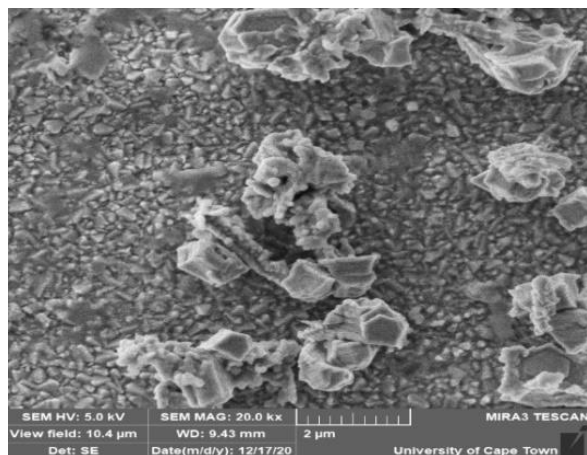


Figure 10: SEM morphology of the films deposited at 2.4 V

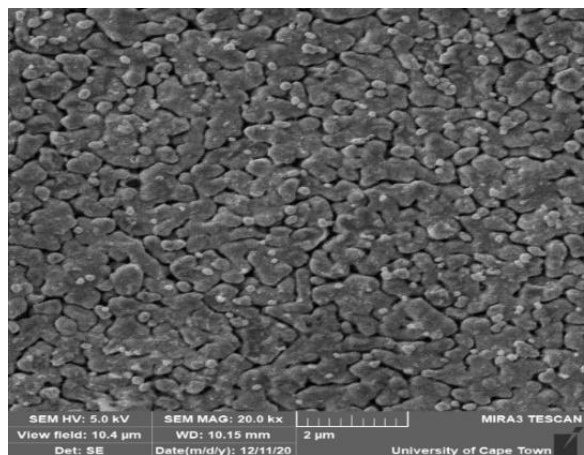


Figure 11: SEM morphology of the films deposited at 2.0 V

#### 4 Conclusion

The optical properties of the electrodeposited CdMnS thin films investigated in this work indicate that the absorbance of the films is high and increases with deposition voltage throughout the Vis & NIR regions of the electromagnetic spectrum. The films transmit moderately in the VIS region while the reflectance is generally low throughout the VIS and NIR regions.

The films also exhibited a high value of absorption coefficient to the order of  $10^4$ - $10^5$   $\text{cm}^{-1}$  throughout VIS and NIR regions which are equally influenced by deposition voltage. The films exhibit a high refractive index value in the range of 2.3 to 2.65 throughout Vis and NIR regions and decrease with an increase in deposition voltage.

The deposited films of CdMnS have wide direct bandgap energy values of 2.6 eV, 2.7 eV, 2.8 eV, 2.7 eV and 2.5 eV and increases with deposition voltage up to 2.0 Volts and thereafter decreased with further increase in deposition voltage. Thin-film thickness analysis showed that the maximum value of the film thickness of 332 nm was obtained at deposition voltage of

2.0 Volts while the minimum thickness of 140 nm obtained at about deposition voltage of 2.26 Volts.

The XRD characterization done on the films showed that the deposited thin films of CdMnS are crystalline with crystallite sizes of 25.54 nm and 16.56 nm for the films deposited at 2.0 V and 2.4 V respectively. The SEM micrograph of the films revealed that the particle size is densely packed on the conductive glass substrate, hence confirming the formation of the deposited thin films.

These properties exhibited by the deposited thin films of CdMnS position them for photovoltaic applications regarding their high absorbance and very low reflectance in the solar spectrum. The range of bandgap energy of the films make the films suitable for photothermal applications and many other electronic and optoelectronic devices that require high temperatures.

#### Acknowledgements

The authors express gratitude to the following scientists and technologist: Whyte G. M., Nsude Kingsley Ugonna, and Nsude Ebere of Nano Research Laboratory, University of Nigeria Nsukka (UNN), Nigeria for their help in carrying out the optical analysis on the samples used in this work. We equally appreciate the team of technologists in the department of Industrial Physics, Chukwuemeka Odumegwu Ojukwu University, Uli, Anambra State, Nigeria, for their assistant during the experimental procedures.

#### Declaration of Competing Interest

The authors declared that there is no conflict of interest during the period of this research work.

#### References

- [1] D. J. Desale, S. Shaikh, F. S. A. Ghosh, R. Birajdar, A. Ghule and R. Sharma, "Effect of annealing on structural and optoelectronic properties of CdS thin film by SILAR method," *Advances in Applied Science Research*, Vol. 2, no. 4, p. 417-425, 2011.
- [2] M. N. Mammadov, A. S. Aliyev and M. Elrouby, "Electrodeposition of cadmium sulfide," *International Journal of Thin Films Science and Technology*, vol. 1, no. 2, p. 42-53, 2012.
- [3] R. Y. Mohammed, S. Abduol and A. M. Mousa, "Structural and Optical properties of Chemically Deposited CdS Thin Films," *International Letters of Chemistry, Physics and Astronomy*, vol. 29, p. 91-104, 2014.
- [4] S. Thanikaikarasan, K. Sundaram, T. Mahalingam, S. Velumani and J. K. Rhee, "Electrodeposition and characterization of Fe doped CdSe thin films from aqueous solution," *Materials Science and Engineering B*, vol. 174, p. 242-248, 2010.



- [5] A. E. Alam, W. M. Cranton and I. M. Dharmadasa, "Electrodeposition of CdS thin-films from cadmium acetate and ammonium thiosulphate precursors," *Journal of Materials Science: Materials in Electronics*, vol. 30, p. 4580-4589, 2019. <https://doi.org/10.1007/s10854-019-00750-1>
- [6] A. N. Nwori, E. I. Ottih, U. V. Okpala and I. Obimma, "Comparative Analysis of Properties of Bamboo Doped and Un-doped Cadmium Sulfide Thin Films Deposited by CBD Method for Possible Applications," *COOU Journal of Physical Sciences*, vol. 1, no. 2, p. 1-10, 2019.
- [7] A. N. Nwori and U. V. Okpala, "Optical Properties of Bamboo Doped Cadmium Sulfide Thin Film for Industrial Applications," *International Journal of Scientific & Engineering Research*, vol. 9, no. 3, p. 1544-1555, 2018.
- [8] F. Iacomi, I. Salaoru, N. Apetroaei, A. Vasile, C. M. Teodorescu and D. Macovei, "Physical characterization of CdMnS nanocrystalline thin films grown by vacuum thermal evaporation," *Journal of Optoelectronics and Advanced Materials*, vol. 8, no. 1, p. 266-270, 2006.
- [9] A. N. Nwori, L. N. Ezenwaka, E. I. Otti, N. A. Okereke and N. L. Okoli, "Optical, Electrical, Structural and morphological Properties of Electrodeposited CdMnS Thin Film Semiconductors for Possible Device Applications," *Journal of Physics and Chemistry of Materials*, vol. 8, no. 2, p. 01-11, 2021.
- [10] J. S. Dargad, "Preparation of  $Cd_{1-x}Mn_xSe$  DMS Thin Films by CBD: Studies on Optical and Electrical Properties," *International Journal of Applied Research (IJAR)*, vol. 1, no. 10, p. 926-932, 2015.
- [11] C. V. V. M. Gopi, M. V. Haritha, S. K. Kim and H. J. Kim, "A strategy to improve the energy conversion efficiency and stability of quantum dot-sensitized solar cells using manganese-doped cadmium sulfide quantum dots," *The Royal Society of Chemistry*, vol. 44, p. 630-638, 2015.
- [12] P. V. Radovanovic, C. J. Barrelet, S. Gradecak, F. Qian and C. M. Lieber, "General Synthesis of Manganese-Doped II-VI and III-V Semiconductor Nanowires," *Nano Letters*, vol. 5, no. 7, p. 1407-1411, 2015.
- [13] P. C. Okafor and A. J. Ekpunobi, "Effect of Manganese Doping Percentage on Band Gap Energy of Cadmium Sulphide (CdS) Nanofilms Prepared by Electrodeposition Method," *International Journal of Science and Research (IJSR)*, vol. 4, no. 12, p. 280-284, 2015.
- [14] M. H. N. Selma, "Optoelectronic Characteristics and Optical Properties of  $Cd_{1-x}Mn_xS$  Nanocrystalline Thin Films Prepared by Chemical Bath Deposition," *International Journal of Application or Innovation in Engineering & Management (IJAIEEM)*, vol. 3, no. 2, p. 329-333, 2014.
- [15] J. S. Dargad and L. P. Deshmukh, " $Cd_{1-x}Mn_xS$  dilute magnetic semiconductor: application in photoelectrochemical cells," *Turkish Journal of Physics*, vol. 33, p. 317-324, 2009.
- [16] A. Hannachi, S. Hammami, N. Raouafi and H. Maghraoui-Meherzi, "Preparation of Manganese Sulfide (MnS) Thin Films by Chemical Bath Deposition: Application of the Experimental Design Methodology," *Journal of Alloys and Compounds*, vol. 663, p. 507-515, 2016.
- [17] M. Karunakaran, S. Maheswari, K. Kasirajan, S. D. Raj and R. Chandramohan, "Structural and Optical Properties of Mn-doped ZnO Thin Films Prepared by SILAR Method," *International Letters of Chemistry, Physics and Astronomy*, vol. 73, p. 22-30, 2017.
- [18] A. N. Nwori, L. N. Ezenwaka, I. E. Ottih, N. A. Okereke, N. S. Umeokwona, N. L. Okoli and I. O. Obimma, "Effect of Deposition Voltage Variation on the Optical Properties of PbMnS Thin Films Deposited by Electrodeposition Method," *Journal of Physics and Chemistry of Materials*, vol. 8, no. 3, p. 12-22, 2021.
- [19] M. D. Jeroh and D. N. Okoli, "Optical and structural properties of amorphous antimony sulphide thin films: Effect of dip time" *Advances in Applied Science Research*, vol. 3, no. 2, p. 793-800, 2012.
- [20] M. H. Suhail and R. A. Ahmed, "Structural, optical and electrical properties of doped copper ZnS thin films prepared by chemical spray pyrolysis technique," *Advances in Applied Science Research*, vol. 5, no. 5, p. 139-147, 2014.
- [21] G. Geetha, P. Murugasen and S. Sagadevan, "Synthesis and Characterization of Manganese Sulphide Thin Films by Chemical Bath Deposition Method," *Acta Physica Polonica*, vol. 132, no. 4, p. 1221-1226, 2017.
- [22] A. Hasnat and J. Podder, "Effect of Annealing Temperature on Structural, Optical and Electrical Properties of Pure CdS Thin Films Deposited by Spray Pyrolysis Technique," *Advances in Materials Physics and Chemistry*, vol. 2, p. 226-231, 2012. <http://dx.doi.org/10.4236/ampc.2012.24034>
- [23] S. M. Salem, N. M. Deraz and H. A. Saleh, "Fabrication and characterization of chemically deposited copper-manganese sulfide thin films," *Applied Physics A*, vol. 126, no. 700, 1-15, 2020. <https://doi.org/10.1007/s00339-020-03883-x>
- [24] A. M. Yahya, Z. F. Mahdi, R. A. Faris and G. H. Mohammed, "Effect of the thickness on the optical properties of nanostructure CuS thin films," *Chemistry and Materials Research*, vol. 6, no. 2, p. 47-54, 2014.
- [25] A. Ait Hssi, L. Atourki, N. Labchir, M. Ouafi, K. Abouabassi, Elfanaoui, A. Ihla and K. Bouabid, "Optical and dielectric properties of electrochemically deposited p-Cu<sub>2</sub>O films," *Material Research Express*, vol. 7, p. 1-9, 2020. <https://doi.org/10.1088/2053-1591/ab6772>

- [26] A. Ohwofosirai, M. D. Femi, A. N. Nwokike, T. O. Joseph, R. U. Osuji and B. A. Ezekoye, "A Study of the Optical Conductivity, Extinction Coefficient and Dielectric Function of CdO by Successive Ionic Layer Adsorption and Reaction (SILAR) Techniques," *American Chemical Science Journal*, vol. 4, no. 6, p. 736-744, 2014.
- [27] N. P. Huse, D. S. Upadhyea, A. S. Dive and R. Sharma, "Study of Opto-Electronic Properties of Copper Sulphide Thin Film Grown by Chemical Bath Deposition Technique for Electronic Device Application," *Invertis Journal of Renewable Energy*, vol. 6, no. 2, p. 74-78, 2016.
- [28] S. Sebastian, I. Kulandaisamy, A. M. S. Arulanantham, S. Valanarasu, A. Kathalingam, A. Jesu Jebathew, M. Shkir and M. Karunakaran, "Influence of Al doping concentration on the opto-electronic properties of SnS thin films realized by NSP," *Optical and Quantum Electronics*, vol. 51, no. 100, p. 1-16, 2019.
- [29] Y. Akaltun, M. A. Yıldırım, A. Ateş and M. Yıldırım, "The relationship between refractive index-energy gap and the film thickness effect on the characteristic parameters of CdSe thin films," *Optics Communications*, vol. 284, p. 2307-2311, 2011.
- [30] L. N. Ezenwaka1, A. N. Nwori, I. E. Ottih, N. A. Okereke and N. L. Okoli, "Investigation of the Optical, Structural and Compositional Properties of Electrodeposited Lead Manganese Sulfide (PbMnS) Thin Films for Possible Device Applications," *Nanoarchitectonics*, vol. 3, no. 1, p. 18-32, 2022.
- [31] B. Papajani, E. Qoku, P. Malkaj, and T. Dilo, "The Study of Phase Compound and the Degree of Crystallinity of Recycled LDPE by X-ray Diffractometer and Optical Microscope," *International Journal of Science and Research (IJSR)*, vol. 4, no. 2, p. 2228-2232, 2015.
- [32] S. Jambaladinni and J. S. Bhat, "Study of Structural, Optical and Dielectric Properties of Mowiol 4-88 (Pva) Filled ZnO Nanocomposites," *Walailak Journal of Science and Technology*, vol. 18, no. 14, p. 1-13, 2021.